Communication over Multipath Fading Channels: A Time-Frequency Perspective

Akbar M. Sayeed and Behnaam Aazhang

Department of Electrical and Computer Engineering
Rice University
6100 South Main Street
Houston, TX 77005, USA

akbar@rice.edu , aaz@rice.edu
Tel: (713) 527-4749
Fax: (713) 524-5237

PIMRC '97, Helsinki, Finland, September 1997.

Abstract

Dynamics of multipath fading have a major effect on the performance of mobile wireless communication systems. The inherently time-varying nature of the mobile wireless channel makes nonstationary signal processing techniques particularly attractive for system design. Time-frequency representations are powerful tools for time-varying signal processing, and in this paper, we present a time-frequency view of wireless communication over multipath channels. Our discussion is anchored on a fundamental finite-dimensional time-frequency representation of the wireless channel that facilitates diversity signaling by exploiting multipath and Doppler shifts. The substantially higher level of diversity afforded by time-frequency processing over conventional techniques translates into significant gains in virtually all aspects of system performance. We illustrate the utility of the time-frequency framework via novel signaling and receiver structures, and multiuser acquisition and interference-suppression algorithms.

Keywords: Fast-Fading, Time-Frequency, Doppler, Multipath, Diversity, RAKE, Acquisition, Interference-Suppression

1 Introduction

The wireless channel has a major effect on the performance of mobile communication systems. The channel is an inherently time-varying system and, for optimal performance, the characteristics of the channel must be incorporated in system design. The time-varying nature of the channel dictates that time-varying signal processing techniques be made to bear on the problem.

Time-frequency representations (TFRs) are powerful tools for the representation and processing of time-varying signals and systems. They are two-dimensional (2D) signal representations jointly parameterized in terms of both time and frequency. As such, TFRs provide a natural framework for representing the time-varying mobile wireless channel, and the optimal signaling and receiver structures for communications over such channels.

In this paper, we present a time-frequency perspective of wireless communications over time-varying multipath channels. Our discussion is primarily in the context of code-division multiple access (CDMA) systems because of their well-known ability to combat multipath fading. Starting with a time-frequency description of the mobile wireless channel, we arrive at a canonical finite-dimensional time-frequency representation of the channel that will serve as the backbone of our treatment.

The canonical time-frequency-based channel representation shows that spread-spectrum signaling over time-varying multipath channels possesses additional degrees of freedom that are not exploited by existing communications systems. Essentially, CDMA systems possess a large time-bandwidth product (TBP) that can be exploited to provide diversity against channel fading. The state-of-the-art RAKE receiver that achieves multipath diversity exploits only the large bandwidth but not the large TBP of CDMA systems. The time-frequency channel representation identifies Doppler as another dimension for diversity, and facilitates the exploitation of joint multipath-Doppler diversity by fully utilizing the available TBP in CDMA systems [1, 2]. Thus, a time-frequency approach to communication over multipath channels has the potential of delivering substantial gains over conventional techniques in virtually all aspects of system performance.

The fundamental time-frequency channel representation can be exploited in a variety of aspects of communication system design and analysis ranging from new signaling and receiver structures to multiuser detection, timing-acquisition and interference-suppression to information-theoretic issues related to multipath fading channels. We illustrate the power of the time-frequency paradigm by focusing on two main themes: 1) novel signaling and receiver structures, and 2) a new approach to multiuser timing-acquisition and interference-suppression that fully incorporates the multipath channel. Our objective is not to give a detailed description of the techniques but to give a flavor for the advantages of the time-frequency approach in the context of the two themes.

The next section briefly introduces TFRs that we use throughout the paper. In Section 3, we provide a natural time-frequency-based description of the mobile wireless channel in the context of CDMA systems, and introduce the canonical time-frequency channel representation. Section 4 describes the basic TFR-based receiver structures that exploit joint multipath-Doppler diversity. In Section 5, we discuss some nontraditional signaling and receiver structures that maximally exploit Doppler diversity. Section 6 leverages the time-frequency receiver structure to propose a near-far resistant framework for multiuser timing acquisition and interference-suppression. Some concluding remarks and avenues for future research are discussed in Section 7.

2 Time-Frequency Preliminaries

TFRs are 2D signal representations in terms of both time and frequency, and are powerful tools for representing time-varying signals and systems. As we will see, TFRs are ideally suited for processing signals transmitted over the inherently time-varying mobile wireless channel.

The concepts of time and frequency shifts play a fundamental role in the theory of TFRs and we will use them throughout the paper. We will denote time and frequency shifts by operators $\mathbf{T}_\tau$ and $\mathbf{F}_\theta$, respectively, defined as

$$(\mathbf{T}_\tau s)(t) \stackrel{def}{=} s(t-\tau) \quad , \quad (\mathbf{F}_\theta s)(t) \stackrel{def}{=} s(t)e^{j2\pi\theta t} \ , \tag{1}$$

where the parameter τ denotes the value of the time-shift, and θ denotes the value of the frequency-shift introduced in the signal.

The TFR of primary interest to us in this paper is the short-time Fourier transform (STFT) which is defined for a signal $s(t)$ as

$$\mathbf{STFT}_s(\theta,\tau;g) \stackrel{def}{=} \int s(t)g^*(t-\tau)e^{-j2\pi\theta t}dt \tag{2}$$

for a given window function $g(t)$. It is a projection of the signal onto a family of functions $\psi_{(\theta,\tau)}$ that are time- and frequency-shifted versions of $g(t)$:

$$\mathbf{STFT}_s(\theta,\tau;g) \stackrel{def}{=} \left\langle s, \psi_{(\theta,\tau)} \right\rangle \tag{3}$$

$$\psi_{(\theta,\tau)}(t) \stackrel{def}{=} (\mathbf{F}_\theta \mathbf{T}_\tau g)(t) = g(t-\tau)e^{j2\pi\theta t} \ , \tag{4}$$

where $\langle \cdot, \cdot \rangle$ denotes the innerproduct. STFT can also be interpreted as a *time-frequency correlation* function. In fact, for each fixed (θ,τ), $\mathbf{STFT}_s(\theta,\tau;g)$ is the matched-correlator output for optimally detecting the time-frequency-shifted signal, $\psi_{(\theta,\tau)} = g(t-\tau)e^{j2\pi\theta t}$, in the presence of additive white Gaussian noise (AWGN); that is, $s(t) = \psi_{(\theta,\tau)}(t) + w(t)$, where $w(t)$ is AWGN. The STFT is an integral part of the time-frequency receivers presented in this paper.

3 The Fundamental Channel Representation

In this section, we introduce the canonical channel representation that is central to our time-frequency framework for CDMA systems. For clarity of exposition, we present the channel representation in terms of the channel-response to a generic spread-spectrum signal. Different signaling and modulation schemes will be introduced in later sections as needed.

Figure 1 shows a schematic of the wireless channel. The complex baseband signal $r(t)$ at the receiver is given by

$$r(t) = s(t) + w(t) \tag{5}$$

where $w(t)$ is the complex AWGN with power spectral density $\mathcal{N}_0$, and $s(t)$ is the channel-transformed version of the transmitted complex baseband signal $x(t)$

$$s(t) = \int h(t,\tau)x(t-\tau)d\tau \ . \tag{6}$$

We are interested in a representation for the time-varying channel [3], described by the kernel $h(t,\tau)$, that maps $x(t)$ into $s(t)$.

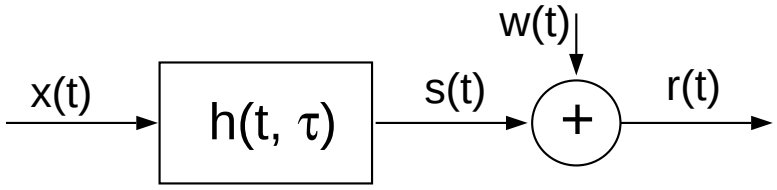

Figure 1: Mobile wireless channel: Linear time-varying system.

It suffices to consider the unmodulated signal to characterize the effects of the channel. Thus, for simplicity of exposition, we consider $x(t) = q(t)$, where $q(t)$ is a spread-spectrum signal of duration T given by

$$q(t) = \sum_{n=0}^{N-1} a[n]v(t - nT_c) \ , \tag{7}$$

where $v(t) = I_{[0,T_c)}(t)$, the chip waveform, T_c is the chip interval, $I_{[a,b)}(t)$ is the indicator function of $[a, b)$, $T = NT_c$, and $a[n]$ is the spreading code (sequence) corresponding to $q(t)$ [4]. The parameter $N \gg 1$ is called the spreading gain of the spread spectrum system. An equivalent representation of the channel which is central to our discussion is in terms of the *spreading function* defined as [3, 4]

$$H(\theta, \tau) \stackrel{def}{=} \int h(t, \tau)e^{-j2\pi\theta t}dt \ . \tag{8}$$

The corresponding representation of $s(t)$ is

$$s(t) = \iint H(\theta, \tau)(\mathbf{F}_\theta \mathbf{T}_\tau q)(t)d\theta d\tau = \iint H(\theta, \tau)q(t - \tau)e^{j2\pi\theta t}d\theta d\tau \ , \tag{9}$$

and thus θ corresponds to the Doppler shifts (frequency-shifts) introduced by the channel (temporal variations), and τ corresponds to the multipath delays (time-shifts). The spreading function $H(\theta, \tau)$ quantifies the time-frequency spreading introduced by the channel. Note from (9) that if we represent the channel by an operator $\mathbf{H}$, it is composed of a linear combination of time- and frequency-shift operators

$$\mathbf{H} = \iint H(\theta, \tau)\mathbf{F}_\theta \mathbf{T}_\tau d\theta d\tau \ . \tag{10}$$

It is well-known that an arbitrary time-varying linear system admits such a representation in terms of time and frequency shifts [5, 6].[1]

3.1 Statistical Channel Parameters

The time-variant channel impulse response $h(t, \tau)$ is best modeled as a stochastic process and a realistic model in many situations is the wide-sense stationary uncorrelated scatterer

[1] The special class of linear time-invariant systems can be represented solely in terms of the time-shift operator which results in the well-known convolution integral.

(WSSUS) model [4, 3] in which the temporal variations in $h(t,\tau)$ are represented as a stationary Gaussian process, and the channel responses at different lags (different scatterers) are uncorrelated (independent). Thus, the channel is characterized by second-order statistics which are given by[2]

$$\mathrm{E}\{H(\theta_1,\tau_1)H^*(\theta_2,\tau_2)\} = \Psi(\theta_1,\tau_1)\delta(\theta_1-\theta_2)\delta(\tau_1-\tau_2)\ , \tag{11}$$

where

$$\Psi(\theta,\tau) \stackrel{def}{=} \mathrm{E}\left\{|H(\theta,\tau)|^2\right\}\ , \tag{12}$$

and $\delta(t)$ denotes the Dirac delta function. The function $\Psi(\theta,\tau) \geq 0$ is called the *scattering function* and denotes the power in the different multipath-delayed and Doppler-shifted signal components. It is particularly useful for describing some salient characteristics of the channel [4, 3]. The maximum range of the values of τ over which $\Psi(\theta,\tau)$ is essentially nonzero is called the *multipath spread* of the channel and is denoted by T_m. Similarly, the maximum range of the θ values over which $\Psi(\theta,\tau)$ is essentially nonzero is called the *Doppler spread* of the channel and is denoted by B_d. In terms of these channel parameters (9) becomes

$$s(t) = \int_0^{T_m}\!\!\int_0^{B_d} H(\theta,\tau)(\mathbf{F}_\theta\mathbf{T}_\tau q)(t)d\theta d\tau = \int_0^{T_m}\!\!\int_0^{B_d} H(\theta,\tau)q(t-\tau)e^{j2\pi\theta\tau}d\theta d\tau\ . \tag{13}$$

Thus, T_m signifies the maximum multipath delay introduced by the channel, and B_d corresponds to the maximum Doppler shift produced by the channel. Note that if there is no time-variation in the channel, then $B_d = 0$; that is, $h(t,\tau) = h(\tau)$, a time-invariant channel.

3.2 The Canonical Channel Representation

The following result describes the fundamental channel representation, obtained by a (θ,τ)-sampling of (13), that plays a central role in our discussion [2, 1].

Theorem 1. If the multipath spread is greater than or equal to the chip period, $T_m \geq T_c$, and the Doppler spread is greater than or equal to the reciprocal to the waveform duration, $B_d \geq 1/T$, then the received signal $s(t)$ in (13) admits the finite-dimensional representation

$$s(t) \approx \frac{T_c}{T}\sum_{l=0}^{L-1}\sum_{p=0}^{P-1}\widehat{H}\left(\frac{p}{T}, lT_c\right)u_{p,l}(t) \tag{14}$$

where $L = \lceil T_m/T_c\rceil$, $P = \lceil B_dT\rceil$, and $\widehat{H}(\theta,\tau)$ is a bandlimited approximation of $H(\theta,\tau)$. The waveforms $u_{p,l}(t)$'s are defined as

$$u_{p,l}(t) \stackrel{def}{=} (\mathbf{F}_{\frac{p}{T}}\mathbf{T}_{lT_c}q)(t) = q(t-lT_c)e^{j\frac{2\pi pt}{T}} \tag{15}$$

and are approximately orthogonal

$$\langle u_{p,l}, u_{p',l'}\rangle \approx \|q\|^2\delta_{p-p'}\delta_{l-l'}\ , \tag{16}$$

where δ_m denotes the Kronecker delta function. □

The (θ,τ)-sampling in (14) is depicted in Figure 2. It is worth noting that there is virtu-

[2]We assume a zero-mean channel (Rayleigh fading). Extension to non-zero mean situations (Rician fading) is straightforward.

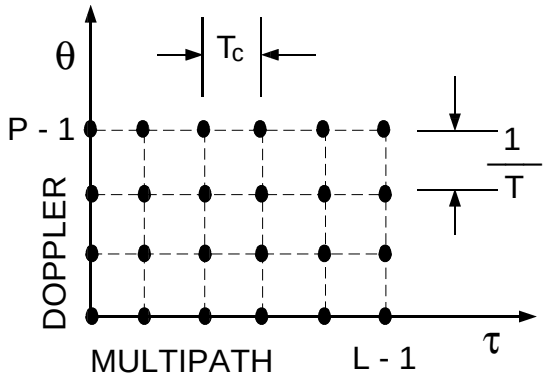

Figure 2: Sampling of the time-frequency plane inherent in the canonical channel representation.

ally no loss of information in the approximate representation (14) due to the (θ, τ)-sampling. The reason is that due to the time- and band-limited nature of the signaling waveform $q(t)$, the receiver only "sees" a corresponding time- and band-limited version ($\widehat{H}(\theta, \tau)$) of the channel ($H(\theta, \tau)$), which in turn justifies the sampling of the spreading function in (14). Note that (14) also implies the following operator representation for the channel as a finite linear combination of time-frequency-shift operators (compare with (10)):

$$\widehat{\mathbf{H}} \approx \frac{T_c}{T} \sum_{l=0}^{L-1} \sum_{p=0}^{P-1} \widehat{H}\left(\frac{p}{T}, lT_c\right) \mathbf{F}_{\frac{p}{T}} \mathbf{T}_{lT_c} \ . \tag{17}$$

The above channel approximation depends on the TBP of the spread-spectrum signal $q(t)$: the larger the TBP, the finer the (θ, τ)-sampling as depicted in Figure 2. We now discuss some useful interpretations and implications of the above representation.

3.3 Discussion

The channel transforms the deterministic (1D) signaling waveform $q(t)$ into a (PL-dimensional) stochastic signal, $s(t)$, as described by (13), and (14) is a canonical representation of $s(t)$. In fact, (14) is a Karhunen-Loève-like expansion of the received signal $s(t)$: the $\widehat{H}(p/T, lT_c)$'s are uncorrelated random variables and the waveforms $u_{p,l}(t)$'s are (roughly) orthogonal. The approximate orthogonality of $\{u_{p,l}(t)\}$ is illustrated in Figure 3 which show a 3D plot of the time-frequency correlation function

$$\mathbf{STFT}_q\left(\frac{p}{T}, lT_c; q\right) = \left\langle q, \mathbf{F}_{\frac{p}{T}} \mathbf{T}_{lT_c} q \right\rangle = \int q(t) q^*(t - lT_c) e^{-j\frac{2\pi pt}{T}} dt \tag{18}$$

of a direct sequence spread-spectrum waveform generated from a length 31 M-sequence [4].

The signal representation (14) also facilitates *diversity signaling* [4] that can be exploited by an appropriate receiver structure (See Sections 4 and 5). Essentially, the orthogonality of the $u_{p,l}(t)$'s implies that they can be processed as separate "channels," and the independence of the $\widehat{H}\left(\frac{p}{T}, lT_c\right)$ implies that those channels can be processed independently to provide diversity [1, 2]. Thus, as depicted in Figure 2, the received signal is resolved into PL

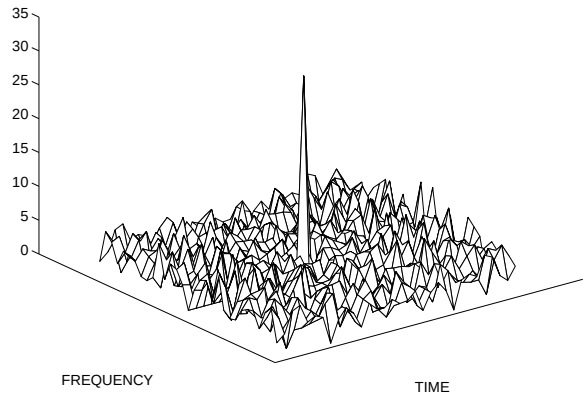

Figure 3: Time-frequency correlation function of a spread spectrum signaling waveform (length-31 M-sequence).

independent multipath-Doppler components (diversity channels) by appropriate sampling of multipath-Doppler (time-frequency) plane.

The diversity signaling is possible due to the large TBP of the spread-spectrum signaling waveform $q(t)$, as is easily evident from Figure 2. The larger the TBP product, the smaller the product $T_c \times \frac{1}{T}$, and the larger the number of delay-Doppler diversity channels. It is worth noting that samples on the multipath axis are due to the large bandwidth and correspond to multipath diversity that is exploited by the conventional RAKE receiver [1, 2, 4]. The samples on the Doppler axis are due to the processing time T and correspond to "Doppler diversity" that is exploited by the "Doppler RAKE" receiver [1, 2]. For maximal channel exploitation both multipath and Doppler diversity should be jointly exploited as is done by the time-frequency-based receiver structures described in Sections 4 and 5.

The canonical signal representation (14) is based on the time-frequency sampling grid depicted in Figure 2. By *fixing* the relative location of the multipath-Doppler components, the grid provides a more parsimonious channel model: assuming perfect synchronization, the channel is completely described by the *number* of multipath-Doppler components and the corresponding channel coefficients — the locations of the different multipath-Doppler components are all known once one is known. Such structure in the channel model is very useful both from a receiver-implementation viewpoint and from an estimation viewpoint. In particular, we will see how this structure yields efficient receiver and signaling designs (Sections 4 and 5), and can be exploited to generate powerful multiuser timing-acquisition and interference-suppression algorithms for multipath channels (Section 6).

4 Basic Diversity Signaling and Reception

In this section, we describe the basic form of the time-frequency receivers that exploit the canonical representation (14) to achieve joint multipath-Doppler diversity in CDMA systems. We restrict our discussion to binary signaling and negligible intersymbol interference. Extensions to M-ary PSK signaling are straightforward, and the effects of intersymbol interference will be discussed in the next section in the context of a signaling scheme employing long overlapping codes.

The complex baseband transmitted signal $x(t)$ in Figure 1 for a continuous data stream can be represented as

$$x(t) = \sum_i q_i(t - iT) \tag{19}$$

where T is the symbol period which is also the duration of the signaling waveform $q_i(t)$, $q_i(t) \in \{q^1(t), q^0(t)\}$, that could either correspond to antipodal signaling ($q^1(t) = -q^0(t)$) or orthogonal signaling ($\langle q^1, q^0 \rangle = 0$). The waveforms $q^m(t),\ m = 0, 1$ are spread-spectrum waveforms of the form (7). Under our assumption of negligible intersymbol interference ($T_m \ll T$), "one-shot" analysis suffices in which each symbol can be treated independently;[3] that is, the i-th symbol is processed using $r(t), (i-1)T \leq t < iT$, only. Thus, without loss of generality, we base our discussion on the $i = 0$ symbol:

$$r(t) = s(t) + n(t) \quad , \quad t \in [0, T). \tag{20}$$

The representation (14) clearly identifies the matched-filter waveforms needed to extract the independent multipath-Doppler components:

$$u_{p,l}^m(t) \stackrel{def}{=} \left(\mathbf{F}_{\frac{p}{T}} \mathbf{T}_{lT_c} q^m\right)(t) = q^m(t - lT_c) e^{j\frac{2\pi pt}{T}} \ , \ p = 0, 1, \cdots, P-1 \ , \ l = 0, 1, \cdots, L-1 \ . \tag{21}$$

Recalling the definition of the STFT in (2), we note that the matched filter outputs can be precisely computed via *sampled* STFTs; that is, the sufficient statistics are given by

$$\left\langle r, u_{p,l}^m \right\rangle \stackrel{def}{=} \mathbf{STFT}_r \left(\frac{p}{T}, lT_c; q^m\right) \ . \tag{22}$$

Figure 4 illustrates the simple implementation of the sampled STFT via a bank of *identical* matched filters determined by the signaling waveforms. The STFT outputs in (22) can be combined to yield optimal coherent and noncoherent receiver structures as described next.

4.1 Coherent Processing

If estimates of the channel coefficients $\widehat{H}(p/T, lT_c)$ are available, such as through a pilot-based channel estimation, coherent processing can be used. The optimal test statistic, which is applicable to both antipodal or orthogonal signaling, is given by

$$\widehat{m}_C = \text{sgn}\left(\text{ real} \left\{ \sum_{l=0}^{L-1} \sum_{p=0}^{P-1} \widehat{H}^* \left(\frac{p}{T}, lT_c\right) \left[\left\langle r, u_{p,l}^1 \right\rangle - \left\langle r, u_{p,l}^0 \right\rangle \right] \right\} \right) \tag{23}$$

where the $u_{p,l}(t)$'s are defined in (21). Figure 5 illustrates the detector structure for coherent processing.

[3] In conjunction with the assumption of negligible intersymbol interference, the conditions of Theorem 1 become: $T_c \leq T_m \ll T$ and $1/T \leq B_d \ll W$, where $W \approx 1/(2T_c)$ is the bandwidth of the signaling waveforms. In Section 5, we relax the condition $B_d \geq 1/T$ by considering signaling based on long, overlapping codes in which block-processing becomes necessary due to intersymbol interference.

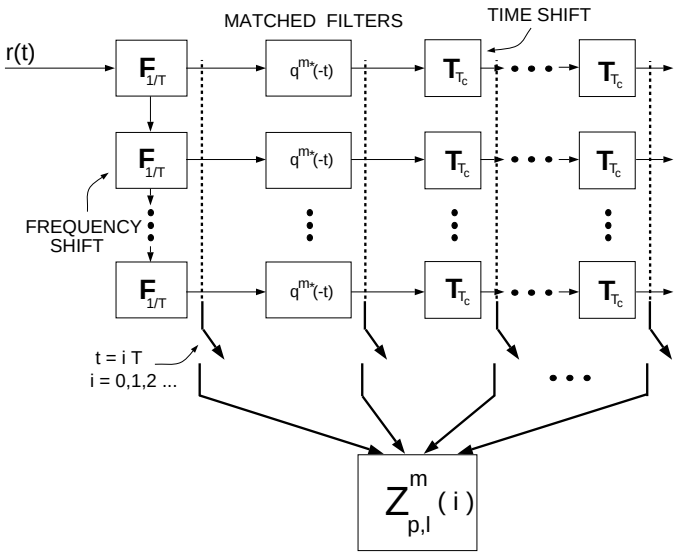

Figure 4: Implementation of sampled STFT using a bank of identical matched filters (signaling waveform). $Z^m_{p,l}(i)$ denotes the sufficient statistics for the i-th symbol; that is, $Z^m_{p,l}(i) = \left\langle r_i, u^m_{p,l} \right\rangle$, where $r_i(t) = r(t + iT)$.

4.2 Noncoherent (Quadratic) Processing

If the actual values of the channel coefficients are not available, noncoherent processing can be used. If the second-order channel statistics ($\Psi(\theta, \tau)$) are known, the optimal noncoherent (quadratic) test statistic can be used which is given by

$$\widehat{m}_{NC} = \mathrm{sgn}\left(\sum_{l=0}^{L-1} \sum_{p=0}^{P-1} \widehat{\Psi}\left(\frac{p}{T}, lT_c\right) \left[\left| \left\langle r, u^1_{p,l} \right\rangle \right|^2 - \left| \left\langle r, u^0_{p,l} \right\rangle \right|^2 \right] \right) \tag{24}$$

where

$$\widehat{\Psi}(\theta, \tau) \stackrel{def}{=} \frac{\|q\|^2 \mathrm{E}\left\{ \left| \widehat{H}(\theta, \tau) \right|^2 \right\}}{\|q\|^2 \mathrm{E}\left\{ \left| \widehat{H}(\theta, \tau) \right|^2 \right\} + \mathcal{N}_0} \,. \tag{25}$$

If the channel statistics are not known, the equal-gain noncoherent combiner can be used which assumes uniform power in the different multipath-Doppler components; that is, $\widehat{\Psi}(\theta, \tau) = 1$. Figure 6 illustrates the quadratic detector structure which is, of course, only applicable with orthogonal signaling.

4.3 Potential Performance Gains

In this section, we demonstrate the potential performance gains of the time-frequency receivers relative to the conventional RAKE receiver that is the state-of-the-art in CDMA systems. The time-frequency receivers are applicable in fast-fading, frequency-selective scenarios and can deliver significant performance gains by exploiting joint multipath-Doppler

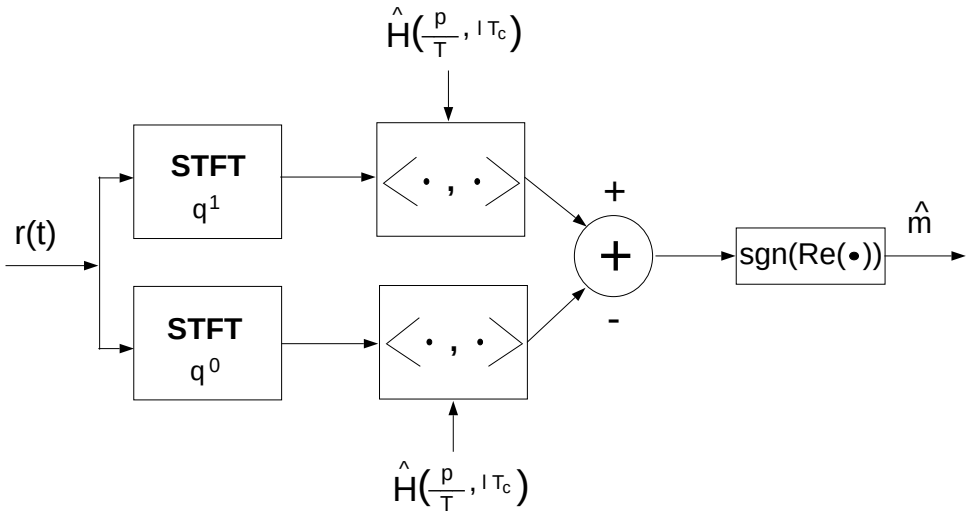

Figure 5: STFT-based coherent detector structure for exploiting joint multipath-Doppler diversity.

diversity. In fact, all time-frequency techniques that are based on the canonical channel representation (14) share the higher level of diversity inherent in the joint multipath-Doppler processing, and are thus capable of exhibiting similar performance gains.

Figure 7 compares the performance of the conventional RAKE receiver to that of time-frequency receiver for $L = 2$ and $P = 2$; that is, one multipath component and one Doppler component are resolvable. All components are assumed to have the same power. Thus, the RAKE corresponds to 2-point diversity, whereas the time-frequency RAKE corresponds to 4-point diversity. The plots in Figure 7 are based on coherent orthogonal signaling and show the bit error probability as a function of SNR for the two receivers.[4] The theoretical curves are based on analytic expressions for probability of bit error [2, 4] and the simulation results are based on 100000 independent experiments that use signaling waveforms based on length-31 M-sequences [1, 2]. Figure 7 clearly show the substantial performance gains achievable with joint time-frequency processing. For example, at $P_e \approx 10^{-4}$, there is a 6dB gain in performance which means that the transmitted power can be reduced by more than a factor of 4 in the case of time-frequency detectors relative to the conventional RAKE.

5 Maximally Time-Selective Signaling and Reception

In this section, we use the fundamental channel representation (14) to propose a new signaling and receiver structure that extends the receivers of the previous section to maximally exploit Doppler diversity. We present an overview of the techniques to provide a flavor of our time-frequency approach. A detailed discussion is provided in [7].

Time-frequency receivers exploit joint multipath-Doppler diversity by utilizing the large TBP of spread-spectrum signaling waveforms via (14). Larger diversity translates into improved receiver performance, and as we noted earlier, the larger the TBP, the larger the

[4]Similar performance gains are obtained for noncoherent processing [1, 2].

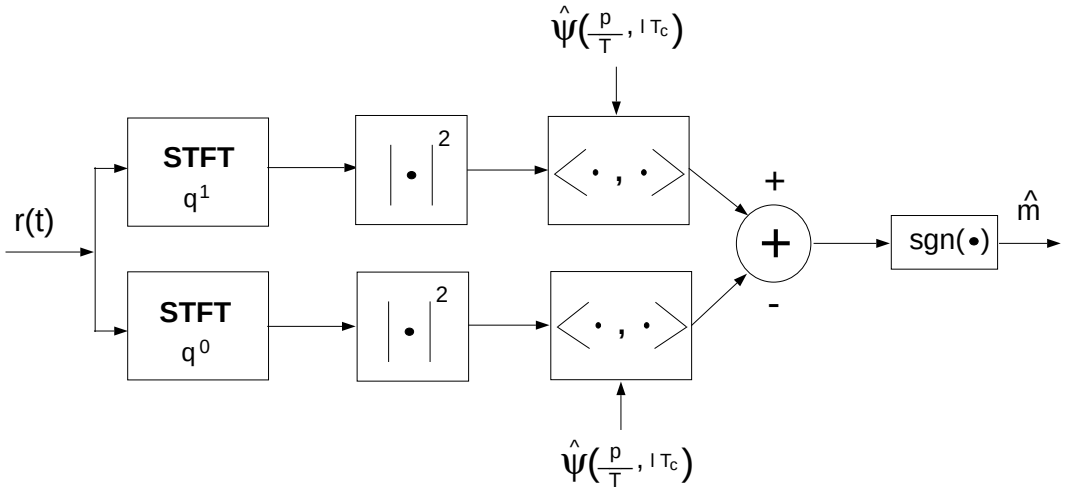

Figure 6: STFT-based quadratic detector structure for exploiting joint multipath-Doppler diversity.

number of achievable diversity components. Clearly, the TBP product can be increased by increasing the bandwidth or the signaling duration or both. The larger bandwidth (smaller T_c) translates into larger diversity due to the larger number of resolvable independent multipath components (see Figure 2). The larger signaling duration (T) achieves higher diversity by resolving a larger number of independent Doppler-shifted signal components (see Figure 2).

In this section, we propose an approach for achieving maximal Doppler diversity by using long signaling waveforms. Consequently, successive symbol waveforms necessarily overlap in time in order to keep the data rate constant, resulting in intersymbol interference. Our methodology shares several features with the approach presented in [8, 9]. However, in contrast to [8, 9], our techniques clearly identify the mechanism — Doppler diversity — by which improved performance is achieved. As such, our framework also provides an alternative, simpler, and intuitively appealing explanation to the ideas presented in [8, 9]. A comparison of our framework with the techniques in [8, 9] is provided in [7].

For simplicity of exposition, we focus on the single-user case using BPSK signaling, and assume perfect synchronization. The results can be extended to the multiuser case [10], and multiuser synchronization issues will be discussed in the next section.

To be consistent with our previous notation, let T denote the duration of the spread-spectrum signaling waveform q, and let T_d denote the symbol period which determines the data rate. Note that in this case $T \gg T_d$, and let $T = DT_d$ for some integer $D \gg 1$, which we refer to as the *overlap factor*. The transmitted baseband signal can be represented as

$$x(t) = \sum_i b(i)q(t - iT_d) \tag{26}$$

which consists of overlapping symbols since $T_d \ll T$. Due to the intersymbol interference, the one-shot detector is no longer sufficient.[5] In fact, it is easy to see that for optimal

[5]However, it may perform satisfactorily under certain conditions. See the discussion later in this section.

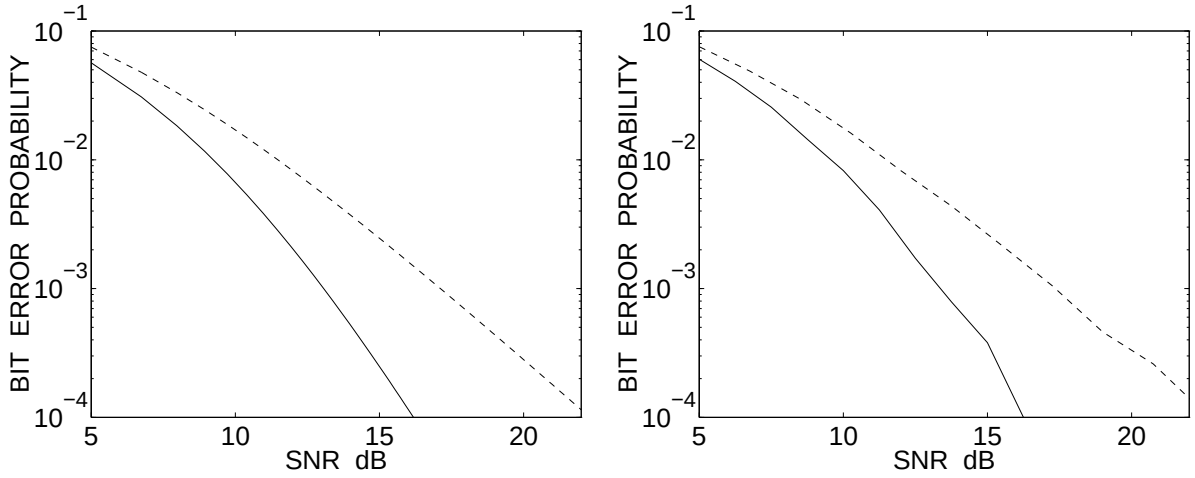

(a) (b)

Figure 7: Performance comparison between conventional RAKE (dashed) versus multipath-Doppler RAKE (solid) for coherent processing. (a) Theoretical. (b) Simulated.

detection all symbols need to be decoded jointly, since at the very least, each symbol overlaps with the preceding and succeeding symbol. Mathematically, this scenario is analogous to asynchronous multiuser detection [11], and intersymbol-interference (ISI) channels [12, 4].

From a practical viewpoint, this entails that a block of symbols has to be decoded jointly. Without loss of generality, assume that we are interested in decoding the 0-th symbol, and consider a block of $2I+1$ symbols centered around it. Thus, the observation interval is $[-IT_d, IT_d + T)$ corresponding to the transmitted waveform

$$x_0(t) = \sum_{i=-I}^{I} b(i) q(t - iT_d) \ , \quad -IT_d \le t < IT_d + T \ . \tag{27}$$

Similarly define $s_0(t)$, $w_0(t)$ and $r_0(t) = s_0(t) + w_0(t)$. Using the canonical representation (14), $s_0(t)$ is given by

$$s_0(t) \approx \frac{T_c}{T} \sum_{i=-I}^{I} b(i) \sum_{l=0}^{L-1} \sum_{p=0}^{P-1} \widehat{H}^i_{p,l} u^i_{p,l}(t) \tag{28}$$

where $\widehat{H}^i_{p,l} \stackrel{def}{=} \widehat{H}^i \left(\frac{p}{T}, lT_c\right)$ are the channel coefficients corresponding to the i-th symbol, and

$$u^i_{p,l}(t) \stackrel{def}{=} (\mathbf{F}_{\frac{p}{T}} \mathbf{T}_{(lT_c + iT_d)} q)(t) = q(t - lT_c - iT_d) e^{j\frac{2\pi pt}{T}} \ . \tag{29}$$

It is evident from (28) that given (estimates of) the channel coefficients, $\widehat{H}^i_{p,l}$, the correlator outputs corresponding to the $u^i_{p,l}(t)$'s are sufficient statistics for the given block of symbols.

It is convenient to introduce a vector notation for the sufficient statistics. Let the correlator outputs be denoted by

$$z^i_{p,l} \stackrel{def}{=} \left\langle r_0, u^i_{p,l} \right\rangle = \left\langle s_0, u^i_{p,l} \right\rangle + \left\langle w_0, u^i_{p,l} \right\rangle \ , \tag{30}$$

where $i = -I, \cdots, I$, $p = 0, \cdots, P-1$, and $l = 0, \cdots, L-1$. By concatenating the $z^i_{p,l}$'s for the different values of the indices l, p, and i (in that order), we can represent the correlator outputs by a $(2I+1)PL \times 1$ vector which we denote by $\mathbf{z}$. Similarly, define the vectors $\mathbf{u}(t)$, $\mathbf{u}^i(t)$ and $\mathbf{u}^i_p(t)$ in terms of the $u^i_{p,l}(t)$'s, and the vectors $\mathbf{h}^i$ and $\mathbf{h}^i_p$ in terms of the scaled channel coefficients $\frac{T_c}{T}\widehat{H}^i_{p,l}$. Finally, define the $(2I+1)PL \times (2I+1)$ matrix $\mathbf{H}$ of channel coefficients as

$$\mathbf{H} \stackrel{def}{=} \begin{bmatrix} \mathbf{h}^{-I} & \mathbf{0} & \cdots & \mathbf{0} \\ \mathbf{0} & \mathbf{h}^{-I+1} & \mathbf{0} & \cdots \\ \vdots & \vdots & \ddots & \vdots \\ \mathbf{0} & \cdots & \mathbf{0} & \mathbf{h}^{I} \end{bmatrix}. \tag{31}$$

With the established notation, the received signal $s_0(t)$ can be represented as

$$s_0(t) = \mathbf{u}^T(t)\mathbf{H}\mathbf{b} \tag{32}$$

where $\mathbf{b}$ is the $(2I+1)\times 1$ vector composed of the bits $b(i)$. Recall that $\mathbf{u}(t)$ is a $(2I+1)PL \times 1$ vector and $\mathbf{H}$ is a $(2I+1)PL \times (2I+1)$ matrix. It follows that the vector $\mathbf{z}$ of correlator outputs can be expressed as

$$\mathbf{z} = \mathbf{R}\mathbf{H}\mathbf{b} + \mathbf{w} \tag{33}$$

where $\mathbf{R}$ is a $(2I+1)PL \times (2I+1)PL$ signal correlation matrix defined as

$$\mathbf{R} \stackrel{def}{=} \int_{-IT_d}^{IT_d+T} \mathbf{u}^*(t)\mathbf{u}^T(t)dt = \begin{bmatrix} \mathbf{R}_{-I,-I} & \mathbf{R}_{-I,-I+1} & \cdots & \mathbf{R}_{-I,I} \\ \mathbf{R}_{-I+1,-I} & \mathbf{R}_{-I+1,-I+1} & \cdots & \mathbf{R}_{-I+1,I} \\ \vdots & \vdots & \vdots & \vdots \\ \mathbf{R}_{I,-I} & \mathbf{R}_{I,-I+1} & \cdots & \mathbf{R}_{I,I} \end{bmatrix} \tag{34}$$

where the $PL \times PL$ matrices $\mathbf{R}_{i,j}$ are defined as

$$\mathbf{R}_{i,j} \stackrel{def}{=} \int_{-IT_d}^{IT_d+T} \mathbf{u}^{i*}(t)\mathbf{u}^j(t)^T \ , \tag{35}$$

and $\mathbf{w}$ is the noise component of $\mathbf{z}$ corresponding to $w_0(t)$ in (30). Evidently, $\mathbf{w}$ is zero-mean, Gaussian-distributed with correlation matrix $\mathcal{N}_0\mathbf{R}$.

The representation of the correlator outputs (sufficient statistics) in (33) is of the same form as in the case of multiuser detection [13, 11] or ISI channels [12, 4]. The optimal receiver [11, 12] requires sequence decoding over the block and suffers from high complexity. For practical implementation, a variety of suboptimal techniques that have been developed for multiuser detection (or ISI channels) may be adapted to this problem [13, 14, 15, 16, 4]. For example, a decorrelating stage [13] (which is equivalent to the zero-forcing solution in ISI channels [4]) may be applied first before coherently combining the various multipath-Doppler components to achieve diversity [10]. A detailed discussion of this approach appears elsewhere [7].

We note that the signaling based on long, overlapping codes proposed above crucially depends on the time-frequency channel representation which is encapsulated in the matrices $\mathbf{H}$ and $\mathbf{R}$. Moreover, since the matrix $\mathbf{R}$ denotes the correlation between the different time-frequency shifted versions of the *same* underlying spreading code, the correlations are not very significant because of the approximate orthogonality property (see Theorem 1). However, for a large value of the overlap factor D, the contributions due to other symbols become significant and must be taken into account [7]. In this context, the approximately "lossless" codes of [8, 9] may be useful as well.

6 Multiuser Timing Acquisition

Thus far, we have explored the time-frequency framework in the single-user case with perfect timing information. As mentioned earlier, the time-frequency approach can be extended to incorporate multiuser detection [10]. In this section, we leverage the fundamental channel representation (14) to address the important problem of multiuser timing acquisition [17]. Our approach offers a powerful alternative to existing multiuser acquisition techniques [18, 19, 20, 21, 22, 23] in that it fully incorporates the multipath channel effects and does not require knowledge of actual channel coefficients thereby resulting in a dramatic reduction in complexity. Moreover, the proposed approach is near-far resistant and is blind in that no training sequence is required. Again, our emphasis is not on details but on how the time-frequency approach can be exploited in the context of acquisition.

6.1 Formulation

Assume BPSK signaling and consider a system of K users so that the received waveform can be expressed as

$$r(t) = \sum_{k=1}^{K} s_k(t - \tau_k) + w(t) \tag{36}$$

where $s_k(t-\tau_k)$ is the received signal corresponding to the k-th user, and τ_k is the corresponding unknown delay relative to some fixed reference. Without loss of generality, we assume that[6]

$$0 \leq \tau_1 \leq \tau_2 \cdots \leq \tau_K \leq T \ . \tag{37}$$

In terms of our channel representation, the signal corresponding to the k-th user can be expressed as

$$s_k(t) \approx \frac{T_c}{T} \sum_i b_k(i) \sum_{l=0}^{L-1} \sum_{p=0}^{P-1} \widehat{H}_{p,l}^{k,i} q_k(t - iT - lT_c) e^{j\frac{2\pi pt}{P}} \tag{38}$$

where $b_k(i)$ denotes the i-th symbol of the k-th user, $\widehat{H}_{p,l}^{k,i} \stackrel{def}{=} \widehat{H}^{k,i}\left(\frac{p}{T}, lT_c\right)$ denote the channel coefficients corresponding to the i-th symbol of the k-th user, and $q_k(t)$ is the spreading waveform of the k-th user. Evidently, we need an observation interval of duration at least $2T$ in order to observe one complete symbol waveform for each user. Thus, without loss of generality, we consider the observation interval $[0, 2T]$ which includes the $i = -1, 0, 1$ symbols for each user.[7]

Conditioned on the bit sequence $b_k(i)$, the received signal $r(t)$ is a zero-mean Gaussian process. Moreover, the correlation function of $r(t)$ is independent of the PSK bit sequence. Thus, the timing acquisition problem can be considered as a problem of estimating the parameters (τ_k) of a Gaussian process.

The correlation function of the received signal $r(t)$ is given by

$$R(t_1, t_2) \stackrel{def}{=} \mathrm{E}\left\{r(t_1) r^*(t_2)\right\} = \sum_{k=1}^{K} R_k(t_1 - \tau_k, t_2 - \tau_k) + \mathcal{N}_0 \delta(t_1 - t_2) \quad , \tag{39}$$

[6] In this section, for simplicity of exposition, we restrict our discussion to nonoverlapping codes of duration T, in contrast to the long overlapping codes of last section.

[7] Longer intervals can be incorporated straightforwardly.

where $R_k(t_1, t_2)$ is the correlation function of $s_k(t)$ given by

$$R_k(t_1, t_2) \approx \frac{T_c^2}{T^2} \sum_i \sum_{p=0}^{P-1} \sum_{l=0}^{L-1} \widehat{\Psi}_{p,l}^k q_k(t_1 - iT - lT_c) q_k^*(t_2 - iT - lT_c) e^{j\frac{2\pi p}{T}(t_1 - t_2)} \tag{40}$$

which follows from (38) where $\widehat{\Psi}_{p,l}^k \stackrel{def}{=} \widehat{\Psi}^k\left(\frac{p}{T}, lT_c\right)$ are the samples of the scattering function for the k-th user.[8] On the space of functions on $[0, 2T)$, denote by $\mathbf{R}_k(\tau_k)$ the operator defined by $R_k(t_1 - \tau_k, t_2 - \tau_k)$:

$$\left(\mathbf{R}_k(\tau_k)x\right)(t) \stackrel{def}{=} \int_0^{2T} R_k(t - \tau_k, u - \tau_k) x(u) du \ . \tag{41}$$

It follows that on the observation interval $[0, 2T)$, the correlation function $R(t_1, t_2)$ admits the operator representation

$$\mathbf{R}(\tau) \stackrel{def}{=} \sum_{k=1}^{K} \mathbf{R}_k(\tau_k) + \mathcal{N}_0 \mathbf{I} \tag{42}$$

where $\mathbf{I}$ denotes the identity operator, and $\tau \stackrel{def}{=} [\tau_1, \tau_2, \cdots \tau_k] \in [0, T)^K$ denotes the unknown vector of timing offsets.[9]

6.2 Maximum Likelihood Approach

The log-likelihood function for the observation waveform $r(t),\ 0 \le t < 2T$, is given by [24]

$$L^\tau(r) = \left\langle \mathbf{R}^{-1}(\tau) r, r \right\rangle - \log\left(\det\left(\mathbf{R}(\tau)\right)\right) \tag{43}$$

where $\det(\cdot)$ denotes the determinant of the operator (product of the eigenvalues).[10] Thus, the maximum-likelihood (ML) estimate of the timing vector τ is given by

$$\tau^{ML} = \arg \max_{\tau \in [0,T)^K} L^\tau(r) \ . \tag{44}$$

From (43), it is clear that finding τ^{ML} is a complicated problem since the nonlinear dependence of $\mathbf{R}^{-1}(\tau)$ on τ cannot be functionally characterized in general, and the likelihood surface will be plagued by many local maxima. Thus, a direct ML approach is not feasible.

Under a weak signal assumption,[11] we can simplify the problem by considering the locally-optimal likelihood function[12] which results in the local ML estimates [24]

$$\tau_k^{LO} = \arg \max_{\tau_k \in [0,T)} \left\langle \mathbf{R}_k(\tau_k) r, r \right\rangle \ , \quad k = 1, 2, \cdots K \ . \tag{45}$$

The estimator in (45) is simple: compute a sequence of quadratic forms for different (quantized) values of $\tau_k \in [0, T)$, and choose the τ_k corresponding to largest value. However, this "decoupled" estimator is clearly not near-far resistant since it does not account for the contribution of the other users in $r(t)$.

[8] Note that under the WSSUS assumption, the channel *statistics* do not change over time.

[9] After appropriate sampling, these operators are represented by matrices over finite dimensional vector spaces.

[10] See also footnote 9.

[11] That is, the SNR for each user is sufficiently low.

[12] The first term in the Taylor expansion of the likelihood function as a function of signal power.

6.3 Interference-Suppression-Based Approach

Both the estimators (44) and (45) are *quadratic* in the observed signal $r(t)$ and represent two extremes: (44) is optimal, requires statistics for all users ($\mathbf{R}(\tau)$) and is computationally intractable, whereas (45) is simple, requires the statistics of only the desired user ($\mathbf{R}_k(\tau_k)$), but is not near-far resistant. Our approach exploits the canonical channel model and strikes a balance between this complexity versus performance trade-off by modifying (45) to be near-far resistant via interference suppression techniques.

For the k-th user, the estimator (45) consists of an array of quadratic processors, $\langle \mathbf{R}_k(\tau_k)r, r\rangle$, each "matched" to a particular value of the delay $\tau_k \in [0, T)$. To suppress the contribution due to other users, we define the optimal quadratic processor for a particular delay τ_k of k-th user as the solution to the following constrained optimization problem

$$\begin{aligned} \mathbf{Q}_k(\tau_k) &= \arg\min_{\mathbf{Q}} \ \mathrm{E}\left\{\langle \mathbf{Q}r, r\rangle\right\} = \arg\min_{\mathbf{Q}} \ \mathrm{Tr}\left(\mathbf{Q}\mathbf{R}(\tau)\right) \\ &\qquad \text{subject to } \mathrm{Tr}\left(\mathbf{Q}\mathbf{R}_k(\tau_k)\right) = 1 \ . \end{aligned} \tag{46}$$

The intuitive motivation for (46) is that the optimal quadratic processor $\mathbf{Q}_k(\tau_k)$ should pass the signal components in the "direction" of the delay τ_k of the k-th user at a fixed gain, while minimizing the contribution due to other signal components (interference). Note that the above optimization problem is similar in spirit to the concept of beamforming in array processing [25], and the linear processor design in [14, 26].

Our algorithm is based on the following characterization of the solution to (46) at the true underlying delay τ_k and under the assumption of no noise. We state the result without proof.

Theorem 2. Consider the noise-free situation; that is, $\mathcal{N}_0 = 0$, $\mathbf{R}(\tau) = \sum_k \mathbf{R}_k(\tau_k)$. At the true underlying delay τ_k of k-th user, the optimal quadratic processor $\mathbf{Q}_k(\tau_k)$ solving (46) is given by[13]

$$\mathbf{Q}_k(\tau_k) = \alpha \sum_{n=1}^{L_k P_k} \mathbf{c}_n \otimes \mathbf{c}_n \tag{47}$$

where $\{c_n(t) : \ t \in [0, 2T), n = 1, 2, \cdots, L_k P_k\}$ are the $L_k P_k$ generalized eigenvectors corresponding to the unit (largest) generalized eigenvalue of the eigenequation

$$\mathbf{R}(\tau)\mathbf{c} = \lambda \mathbf{R}_k(\tau_k)\mathbf{c} \ , \tag{48}$$

L_k and P_k are the number of multipath and Doppler components, respectively, in the channel representation (14) for user k, and α is chosen to satisfy the constraint in (46). □

Inspired by the above result, the basic idea behind our algorithm is to quantize the interval $[0, T)$ into intervals of length $T_c/2$, as done in [23], and set up a multihypothesis testing problem corresponding to the different quantized values of the timing-offset τ_k of the desired user k. Once τ_k has been determined to within half a chip interval, finer quantization can be used to improve the estimate. The essential generic steps are outlined below.

Timing Acquisition Pseudo-Algorithm:
Step 1. Let $I = 2N + 1$, where $T = NT_c$. Define

$$\tau_k(i) = \frac{T_c}{2} i \ , \quad i = 0, 1, \cdots, I - 1 \ . \tag{49}$$

[13]The notation $\mathbf{c}_n \otimes \mathbf{c}_n$ denotes a rank-1 projection operator defined as $((\mathbf{c}_n \otimes \mathbf{c}_n)x)(t) \stackrel{def}{=} \int c(t)c^*(u)x(u)du$.

Step 2. For each i, compute $\mathbf{Q}_k(\tau_k(i))$ via (47) corresponding to the L_kP_k largest generalized eigenvalues of

$$[\mathbf{R}(\tau) - \mathcal{N}_0\mathbf{I}]\,\mathbf{c} = \lambda\mathbf{R}_k(\tau_k(i))\mathbf{c}\ . \tag{50}$$

Step 3. Estimate the delay τ_k as

$$\widehat{\tau}_k = \tau_k(i_{max}) = \arg\max_{\tau_k(i)} \mathrm{Tr}\left(\mathbf{Q}_k(\tau_k(i))[\mathbf{R}(\tau) - \mathcal{N}_0\mathbf{I}]\right)\ , \tag{51}$$

or as based on a hypothesis test on the closeness of the L_kP_k largest generalized eigenvalues of (50) to unity (see Theorem 2).
Step 4. Get a refined estimate by further quantizing the $T_c/2$ interval determined by i_{max} and the neighboring index yielding the larger (smaller) metric in Step 3. □

6.4 Discussion

To apply the acquisition algorithm in practice, $\mathbf{R}(\tau)$ and $\mathcal{N}_0$ can be estimated from received data. The correlation function $\mathbf{R}_k(\tau_k)$ corresponding to the desired user k is determined by the canonical channel representation and is given by (40). In the absence of knowledge about the channel statistics, $\Psi^k_{p,l} = 1$ may be used.

The most attractive feature of the proposed approach is that it incorporates the canonical time-frequency channel representation in the acquisition algorithm without having to estimate the channel coefficients, thereby dramatically reducing the complexity. Due to the quadratic processing, the channel is represented via its second-order statistics which can be reliably estimated or approximated. The near-far resistance of the algorithm essentially stems from Theorem 2 which states that after accounting for the effects of noise, the best quadratic processor for the desired user (corresponding to the correct delay) is independent of the power of other users. Details of this approach appear elsewhere [27].

We note that our acquisition approach is equally applicable in slow fading situations in which we can ignore the Doppler aspects. Moreover, once the timing has been acquired, a near-far resistant linear or quadratic time-frequency equalizer can be designed along the lines of [10] or [14, 26]. Finally, even though we have discussed timing acquisition, our framework can be readily extended to incorporate (carrier) frequency acquisition as well.

7 Conclusion

Central to modern mobile communication networks is the fast-fading multipath wireless channel that is one of the single most important factors affecting the system performance. For optimal processing, time-varying signal processing techniques are needed to account for the inherently time-varying dynamics of the channel. We have provided a time-frequency framework for mobile wireless communications that emphasizes this time-varying perspective. The signal processing tools underlying our framework are TFRs that perform joint time-frequency processing.

At the heart of our framework is a canonical finite-dimensional time-frequency representation of the channel in terms of time (multipath) and frequency (Doppler) shifts of the transmitted signal. The fundamental channel representation not only provides new insights but also leads to new design strategies that can deliver significantly improved performance due to joint multipath-Doppler diversity signaling.

The multipath-Doppler diversity inherent in our time-frequency framework is achieved by exploiting the large TBP of spread-spectrum signaling waveforms in CDMA systems. The

conventional RAKE receiver only utilizes the large bandwidth to achieve multipath diversity. The additional Doppler diversity afforded by joint time-frequency processing translates into substantial performance gains in virtually every aspect of system design.

Doppler diversity is essentially achieved by doing processing over sufficiently long time intervals so that the effective channel becomes time-selective. In Section 5 we presented the basic ideas behind a novel signaling scheme in which long overlapping spreading waveforms are used to achieve long processing times. A promising direction for future research is the use of block processing to achieve Doppler diversity via some form of sequence decoding. Such a scheme could be applicable in existing systems such as the IS-95 standard in which a block of 200 symbols is processed together for the purpose of interleaving [28].

In addition to novel signaling and receiver structures, the canonical time-frequency channel representation can be leveraged in several other aspects of system design. In particular, in Section 6 we developed a framework for multiuser timing-acquisition based on quadratic processing. The acquisition framework incorporates the multipath fading channel and fully exploits the signal structure provided by the canonical time-frequency representation. Moreover, the approach can be extended to provide near-far resistant algorithms for joint multiuser acquisition and demodulation over multipath fading channels [10, 27].

The fundamental time-frequency-based signal representation also has a curious connection to the "spreading versus coding" ideas of Massey [29]. As such, our representation suggests that the channel provides a form of coding via multipath-Doppler signaling. An interesting research issue is the exploration of this connection to quantify the advantages of CDMA systems in the context of multipath fading.

In short, our time-frequency approach provides a unified signal processing framework for communication over multipath fading channels. It ties in with several existing approaches, suggests new design strategies, provides intuitively appealing alternatives to others, and leads to several new insights and directions for future research that could prove quite fruitful.

References

[1] A. M. Sayeed and B. Aazhang, "Exploiting Doppler diversity in mobile wireless communications," in *Proc. 1997 Conf. Inf. Sci. Syst. (CISS'97)*, 1997.

[2] A. M. Sayeed and B. Aazhang, "Joint multipath-Doppler diversity in mobile wireless communications," *to appear in the IEEE Trans. Commun.*

[3] P. A. Bello, "Characterization of randomly time-variant linear channels," *IEEE Trans. Commun. Syst.*, vol. CS-11, pp. 360–393, 1963.

[4] J. G. Proakis, *Digitial Communications*. New York: McGraw Hill, 3rd ed., 1995.

[5] R. G. Shenoy and T. W. Parks, "The Weyl correspondence and time-frequency analysis," *IEEE Trans. Signal Processing*, vol. 42, pp. 318–332, Feb. 1994.

[6] W. Kozek, "Time-frequency signal processing based on the Wigner-Weyl framework," *Signal Processing*, vol. 29, pp. 77–92, Oct. 1992.

[7] S. Bhasyam, A. M. Sayeed, and B. Aazhang, "Time-selective signaling and reception in for fading channels," *in preparation.*

[8] G. W. Wornell, "Spread-signature CDMA: Efficient multiuser communications in the presence of fading," *IEEE Trans. Inform. Theory*, vol. IT-41, pp. 1418–1438, Sep. 1995.

[9] G. W. Wornell, "Spread-response precoding for communication over fading channels," *IEEE Trans. Inform. Theory*, vol. IT-42, pp. 488–501, Mar. 1996.

[10] A. M. Sayeed, A. Sendonaris, and B. Aazhang, "Multiuser detectors for fast-fading multipath channels," in *Proc. 31st Asilomar Conf. Signals, Syst., and Computers*, 1997.

[11] S. Verdu, "Minimum probability of error for asynchronous Gaussian multiple-access channels," *IEEE Trans. Inform. Theory*, vol. IT-32, pp. 85–96, Jan. 1986.

[12] G. D. Forney, "Maximum likelihood sequence estimation of digital sequences in the presence of intersymbol interference," *IEEE Trans. Inform. Theory*, vol. IT-18, pp. 363–378, May 1972.

[13] R. Lupas and S. Verdu, "Near-far resistance of multiuser detectors in asynchronous channels," *IEEE Trans. Commun.*, vol. 38, pp. 496–508, Apr. 1990.

[14] U. Madhow and M. L. Honig, "MMSE interference suppression for direct-sequence spread-spectrum CDMA," *IEEE Trans. Commun.*, vol. 42, pp. 3178–3188, Dec. 1994.

[15] A. Duel-Hallen, "Decorrelating decision-feedback multiuser detector for synchronous code-division multiple-access channel," *IEEE Trans. Commun.*, vol. 41, pp. 285–290, Feb. 1993.

[16] M. K. Varanasi and B. Aazhang, "Multistage detection in asynchronous code-division multiple-access communications," *IEEE Trans. Commun.*, vol. 38, pp. 509–519, Apr. 1990.

[17] U. Madhow and M. Pursley, "Acquisition in direct-sequence spread-spectrum communication networks: an asymptotic analysis," *IEEE Trans. Inform. Theory*, vol. IT-39, pp. 903–912, May 1993.

[18] S. Y. Miller and S. C. Schwartz, "Parameter estimation for asynchronous multiuser communincation," in *Proc. 1989 Conf. Inform. Sci. Syst. (CISS'89)*, pp. 294–299, 1989.

[19] S. E. Bensley and B. Aazhang, "Subspace-based channel estimation for code division multiple access communication systems," *IEEE Trans. Commun.*, vol. 44, pp. 1009–1020, Aug. 1996.

[20] A. Radovic and B. Aazhang, "Iterative algorithms for joint data detection and delay estimation for code division multiple access communication systems," in *Proc. 31st Ann. Allerton Conf. Commun., Contr., Computing, Monticello, IL*, pp. 1–10, 1993.

[21] R. F. Smith and S. L. Miller, "Code timing estimation in a near-far environment for direct-sequence code-division multiple-access," in *Proc. Milcom '94*, pp. 47–51, 1994.

[22] E. G. Strom, S. Parkvall, S. L. Miller, and B. E. Ottersten, "Propagation delay estimation in asynchronous direct-sequence code-division multiple access systems," *IEEE Trans. Commun.*, vol. 44, pp. 84–93, Jan. 1996.

[23] U. Madhow, "Blind adaptive interference suppression for the near-far resistant acquisition and demodulation of direct-sequence CDMA systems," *IEEE Trans. Signal Processing*, vol. 45, pp. 124–136, Jan. 1997.

[24] H. V. Poor, *An Introduction to Signal Detection and Estimation*. Springer-Verlag, 1988.

[25] B. D. Van Veen and K. M. Buckley, "Beamforming: A versatile approach to spatial filtering," *IEEE Signal Processing Magazine*, pp. 4–24, Apr. 1988.

[26] M. L. Honig, U. Madhow, and S. Verdu, "Blind adaptive multiuser detection," *IEEE Trans. Inform. Theory*, vol. IT-41, pp. 944–960, July 1995.

[27] A. M. Sayeed and B. Aazhang, "Noncoherent multiuser timing acquisition over multipath fading channels," *in preparation.*

[28] T. S. Rappaport, *Wireless Communications.* New Jersey: Prentice Hall, 1996.

[29] J. L. Massey, "Towards an information theory of spread-spectrum systems," in *Code Division Multiple Access Communications* (S. G. Glisic and P. A. Lippänen, eds.), pp. 29–46, Kluwer, 1995.